Metrology in the presence of thermodynamically consistent measurements

Muthumanimaran Vetrivelan,[1] Abhisek Panda,[1] and Sai Vinjanampathy[1,2,3,*]
[1]*Department of Physics, Indian Institute of Technology-Bombay, Powai, Mumbai 400076, India*
[2]*Centre of Excellence in Quantum Information, Computation, Science and Technology, Indian Institute of Technology Bombay, Powai, Mumbai 400076, India*
[3]*Centre for Quantum Technologies, National University of Singapore, 3 Science Drive 2, Singapore 117543*

(Received 30 May 2023; accepted 19 March 2024; published 6 May 2024)

Thermodynamically consistent measurements can preserve either statistics (unbiased) or marginal states (noninvasive) but not both. Here we show the existence of metrological tasks which unequally favor each of the aforementioned measurement types. We consider two different metrology tasks, namely, the weak value amplification technique and repeated metrology without resetting. We observe that unbiased measurement is better than noninvasive measurement for the former and the converse is true for the latter. We provide finite-temperature simulations of transmon sensors which estimate how much cooling, a resource for realistic measurements, is required to perform these metrology tasks.

DOI: 10.1103/PhysRevA.109.052610

I. INTRODUCTION

Quantum metrology employs nonclassical resources for tasks such as parameter estimation [1–3], state discrimination [4,5], and hypothesis testing [5]. The sensitivity of a metrological task achieves quantum advantage based on the nonclassical resources in probe states and the choice of measurement. Generally, such probe states are considered to be pure, and measurements are considered to be ideal. In the experiment, the probe states and measurement device are at finite temperatures. This implies that preparing a pure state consumes infinite thermodynamic resources [6–10]. As a consequence, two varieties of realistic measurements emerge, namely, unbiased (UB) and noninvasive (NI) measurements [11]. Incorporating these thermal resources in realistic metrology requires further study.

Hence, a natural question that arises for a given metrological task is which type of realistic measurement is more suitable. We answer by studying the utility of nonideal measurements on different metrological schemes. It is known that a UB measurement protects the statistics and a NI measurement protects the postmeasurement state [11]. Here we show that a task that places a premium on statistics prefers the UB measurement, and a task for which the postmeasurement state is important prefers the NI measurement. First, we briefly review nonideal measurements. We then provide the aforementioned examples and analyze why a measurement type is preferred over another. Finally, we summarize and discuss our results.

II. NONIDEAL MEASUREMENT

Following von Neumann [12] and Lüder [13], measurements and the role that pointers play in the act of measurement have garnered intense interest. This has led to the idea of nonideal measurements, which was studied extensively in [11,14,15]. In this paper we briefly review the properties of ideal measurements and discuss why such measurements are not feasible following the work of [11].

Consider the quantum system to be in state ρ_S and the measuring device (pointer) ρ_P. To make an ideal measurement on the system, the eigenstates of the system observable $\{|i\rangle\}$ are correlated to the orthogonal states of a pointer $\{|\psi_n^i\rangle\}_n$. This is done by jointly evolving the system and pointer from state $\rho_S \otimes \rho_P \to \rho_{SP}$. Following this, a projective measurement is performed on the pointer using $\Pi_i = \sum_n |\psi_n^i\rangle\langle\psi_n^i|$, and the system state is inferred. If the correlation is perfect and the pointer is observed in $|\psi_n^i\rangle$, we conclude that the system is in state $|i\rangle$. Such ideal measurements have three fundamental properties, namely, *unbiasedness, noninvasiveness*, and *faithfulness* [11]. A measurement is said to be nonideal if any one of the properties is not satisfied.

The *unbiased* property states that the premeasurement statistics of the system are accurately reflected by the postmeasurement pointer statistics, i.e.,

$$\mathrm{Tr}[\mathbb{I} \otimes \Pi_i \rho_{SP}] = \mathrm{Tr}[|i\rangle\langle i|\rho_S] \;\; \forall\, i, \rho_S. \tag{1}$$

The second property desired for ideal measurements is *noninvasiveness*. This property says that the measurement interaction should not change the measurement statistics for the system, namely,

$$\mathrm{Tr}[|i\rangle\langle i| \otimes \mathbb{I}\, \rho_{SP}] = \mathrm{Tr}[|i\rangle\langle i|\rho_S] \;\; \forall\, i, \rho_S. \tag{2}$$

Finally, a measurement is *faithful* if there is a one-to-one correspondence between the pointer outcome and the postmeasurement system state, namely,

$$C(\rho_{SP}) = \sum_i \mathrm{Tr}[|i\rangle\langle i| \otimes \Pi_i \rho_{SP}] = 1. \tag{3}$$

This property suggests there should be perfect correlation between system eigenstates $\{|i\rangle\}$ and pointer states

*sai@phy.iitb.ac.in

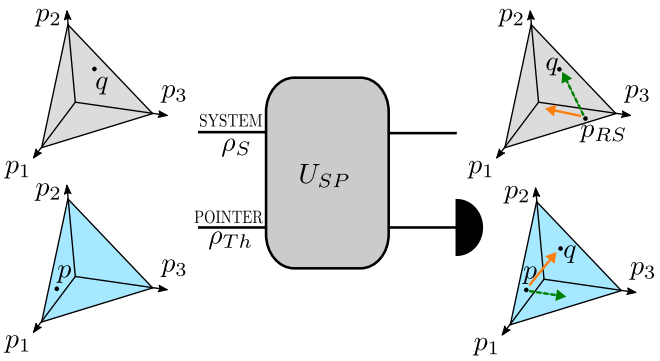

FIG. 1. An illustration of the change in the probabilities of the system and pointer states in a fixed basis across a measurement as described in the text. The probability vector associated with the system statistics (gray) and that for the pointer (blue) are shown across a correlating unitary followed by a measurement. In the space of the system statistics, the statistics p_{RS} of the reduced state is the same as the system statistics q for NI measurements (green dashed line) and points to a different probability vector for UB measurements (orange solid line). In the case of the pointer, the pointer statistics p correctly points to q for UB but not for NI.

$\{|\psi_n^i\rangle\}_n$. Such measurements are possible only if $\mathrm{rank}(\rho_{\mathrm{P}}) \leqslant \dim(\rho_{\mathrm{P}})/\dim(\rho_{\mathrm{S}})$ [11]; i.e., an ideal measurement requires a non-full-rank pointer state. As the laws of thermodynamics forbid the preparation of a non-full-rank state with finite resources, a realistic measurement is always nonideal. At finite temperature, the system and the pointer evolve jointly to get maximum faithfulness, but the correlation will not be perfect [$C(\rho) < 1$]. A measurement cannot be unbiased and noninvasive because both properties together would also imply faithfulness [11,16]. Hence, a maximally faithful measurement can either be unbiased or noninvasive. The UB measurement replicates the system statistics through the pointer but changes the statistics of the reduced system after measurement. As a result, the system needs to be discarded or reset to measure again. On the other hand, the NI measurement preserves the statistics of the system in the reduced system state postmeasurement at the expense of the pointer statistics being different from the system statistics, which is shown in Fig. 1. These properties associated with different nonideal measurements make them favorable in different scenarios. To compare the effect of nonideal measurements in a metrological task, we identify a figure of merit and use it to discuss cases in which each measurement type is favored.

In local quantum metrology the Fisher information has been identified as the figure of merit [17,18]. Given the convexity of the Fisher information, this figure of merit is maximum for ideal optimal measurements on pure states. It should be noted that the convexity of the quantum Fisher information does not imply that generic pure states have more Fisher information than generic mixed states. Consider the following example in which the system is initialized in the pure state $|0\rangle$ and evolved with $U = e^{i\theta\sigma_z}$; the final state has no parameter encoded in it and has zero Fisher information. For generic nonmaximally mixed states with finite coherence, the corresponding quantum Fisher information is always greater than zero. To formalize the role of purity, let us consider a density matrix represented as a generalized Bloch vector. Unitary parametrization encodes the parameter by rotating the generalized Bloch vector. While holding the direction of the Bloch vector constant, we can show that the quantum Fisher information for unitary parametrization is monotonous to the purity (see Appendix A). Hence, given the choice between two states with different purities but with generalized Bloch vectors pointing in the same direction, we will get more Fisher information from the state with higher purity. This is one of the key intuitions of this paper.

The final observation is that states on a generalized Bloch sphere lose their length while preserving their direction as temperature is increased. Hence, it follows that for generic thermal maps parameterized by temperature, increasing the temperature reduces the underlying quantum Fisher information. The purity of the system states is not the only issue with quantum metrology in the presence of finite resources. If we presuppose mixed initial states but pure pointer states, then measurements that saturate the quantum Fisher information are plausible. Given the fact that such pure-state pointers also violate the third law, we can conclude that the classical Fisher information associated with any given mixed-pointer state and any optimal measurement will still be less than the corresponding quantum Fisher information. Hence, it is important to understand the role of the two measurement schemes outlined in [11] for quantum metrology.

The two thermodynamically consistent measurements discussed above can either preserve reduced system statistics or reveal system statistics through the pointer. According to the figure of merit, if revealing system statistics is more important than preserving reduced system statistics, the UB measurement is favored over the NI measurement. In Sec. III, we show this by considering an example by applying nonideal measurements with weak value amplification (WVA), where the figure of merit is the postselected Fisher information. On the other hand, if preserving reduced system statistics leads to a higher postmeasured pointer purity than revealing the system statistics, then the NI measurement is favored over the UB measurement. This is discussed in Sec. IV by considering an example of a repeated metrological scheme without resetting.

III. WEAK VALUE AMPLIFICATION FAVORS UNBIASED MEASUREMENTS

WVA is a metrological scheme that uses postselection to amplify small signals [19]. It involves preparing quantum states and postselecting the evolved state in a specific final state. It has a well-known trade-off between postselection probability and amplified weak value [20]. Although rejected measurements leave out some quantum information [21], WVA has demonstrated better metrological performance in the presence of certain noises [22]. WVA has proven useful in disparate experiments, such as amplifying optical nonlinearities [23], measuring ultrasmall time delays of light [24], detector saturation, and measuring low frequencies [25], maintaining its relevance in modern quantum metrology. From a thermodynamic perspective, the reliance of WVA on pure states precludes us from implementing it in finite-dimensional physical systems, as explained below. We hence investigate WVA with constraints in the preparation of states

and realistic nonideal measurements. For this reason, we summarize WVA in a way that readily generalizes to mixed states.

The parameter g is coupled through system A and an ancilla degree of freedom known as *meter* B via the Hamiltonian $H = gA \otimes B$. We note that this meter degree of freedom accumulates the effect of postselection and is separate from the pointer introduced to model thermodynamic resource costs of performing measurements. The system and meter are prepared in an initial state $\rho_s \otimes \rho_m$ and are evolved for a short time τ, where $g\tau \ll 1$ under the influence of the Hamiltonian above. The system is postselected by a nearly orthogonal pure state $|\psi_f\rangle$ (generalized below to mixed states), such that the average of the expected spin can be larger than the mean:

$$\mathcal{A}_{\rm w} = \frac{\langle\psi_f|A\rho_s|\psi_f\rangle}{\langle\psi_f|\rho_s|\psi_f\rangle} = \frac{\langle\psi_f|A\rho_s|\psi_f\rangle}{P_s}. \tag{4}$$

This effectively evolves the meter state as $\exp(-ig\tau\mathcal{A}_{\rm w}B)\rho_m \exp(ig\tau\mathcal{A}_{\rm w}B)$. The postselection of the system state in $|\psi_f\rangle$ depends on a projective measurement onto a pure state, which, as noted above, is thermodynamically inconsistent.

To include the effect of nonideal measurements, we introduce a pointer degree of freedom. Our setup consists of three parts, i.e., a system ρ_S of dimension d_S, a meter ρ_m of dimension d_m, and a pointer ρ_P of dimension d_P. The system and pointer are governed by local Hamiltonians H_S and H_P, respectively, where

$$H_S = E_S|\psi_i^\perp\rangle\langle\psi_i^\perp|, \quad H_P = E_P|\psi_f^\perp\rangle\langle\psi_f^\perp|. \tag{5}$$

To postselect the system through a pointer, the dimension of the pointer should be an integer multiple of the system. The system is weakly correlated to the meter and strongly correlated to the pointer. The strong projective measurement and postselection by the pointer gives the amplified reading in the meter. To simulate nonideal measurement we prepare the initial system and pointer in a thermal state,

$$\begin{aligned}\rho_S &= q|\psi_i\rangle\langle\psi_i| + \bar{q}|\psi_i^\perp\rangle\langle\psi_i^\perp|,\\ \rho_P &= p|\psi_f\rangle\langle\psi_f| + \bar{p}|\psi_f^\perp\rangle\langle\psi_f^\perp|,\end{aligned} \tag{6}$$

where $\bar{q}/q = e^{-\beta E_S}$, $\bar{p}/p = e^{-\beta E_P}$, and $\beta = 1/\mathrm{T}$. Here we choose $d_S = d_P = 2$, but it should be noted that the result can be generalized to any values of $d_S \geqslant 2$ and $d_P \geqslant 2$. Prior to performing a measurement, we correlate the system and pointer in the measurement basis using a suitable unitary matrix. To perform a suitable NI (UB) measurement, we use $U_{\rm corr} = I_m \otimes \sum_j |j\rangle\langle j| \otimes \tilde{U}^j$ ($U_{\rm corr} = I_m \otimes \sum_{ij} |i\rangle\langle j| \otimes |j\rangle\langle i|\tilde{U}^j$). The unitary $\tilde{U}_j$ is adjusted such that the measurement is maximally faithful. The nonideal measurement is then simulated by doing a projective measurement on the pointer, which is an instance of our *Heisenberg's cut* [26]. Given that the pointer is not pure, the desired near-orthogonal projection of the system state happens probabilistically; the other outcome is less favorable and is governed by the nonzero-temperature pointer. This causes the postselected meter state to be a convex mixture of two outcomes, one which we term the *true positive* (kicked state) and one which we label the *false-positive state*. This is given by

$$\rho_m^{PS({\rm NI})} = (pqP_s + \bar{p}\bar{q}P_s)\eta_1 + (p\bar{q}\bar{P}_s + \bar{p}q\bar{P}_s)\eta_2. \tag{7}$$

Here $\eta_1 = \exp(ig\mathcal{A}_{\rm w}B)\rho_m \exp(-ig\mathcal{A}_{\rm w}B)$ is the weak value amplified meter state, and $\eta_2 = \exp(ig\mathcal{A}_{\rm w}^\perp B)\rho_m \exp(-ig\mathcal{A}_{\rm w}^\perp B)$ is the nonamplified meter state, where

$$\mathcal{A}_{\rm w}^\perp = \frac{\langle\psi_f^\perp|A\rho_s|\psi_f^\perp\rangle}{\langle\psi_f^\perp|\rho_s|\psi_f^\perp\rangle}. \tag{8}$$

A detailed calculation of the kicked state is given in Appendix B. Likewise, for the unbiased measurement, the postselected meter state will be

$$\rho_m^{PS({\rm UB})} = qP_s\eta_1 + \bar{q}\bar{P}_s\eta_2. \tag{9}$$

As $\mathcal{A}_{\rm w}^\perp \ll \mathcal{A}_{\rm w}$, we can approximate $\eta_2 \approx \rho_m$. The postselected states in Eqs. (7) and (9) will have reduced amplification compared to the ideal scenario.

From Eq. (9), we can see that the trade-off between the postselection probability and amplified weak value implied in Eq. (4) still persists. This trade-off further depreciates in Eq. (9) because the initial state is prepared in the mixed state and nonideal measurements for postselection are performed. In addition, another variety of trade-off is represented by the fact that postselection implies that some measurements outcomes are ignored. Measuring the system in a rarely postselected state and ignoring other possible final states leads to discarding potential information available from the system. This leads to suboptimal information-theoretic performance of the WVA scheme compared to the conventional scheme in which the information from all possible final states is collected. To measure performance in the ideal scenario, the quantum Fisher information for the postselected scheme $\mathcal{I}_{\rm PS}(g)$ and the total quantum Fisher information $\mathcal{I}(g)$ due to the initial state are compared. Hence, the quantum Fisher information obtained with the WVA scheme will always be less than $\mathcal{I}(g)$, and the ratio $\mathcal{I}_{\rm PS}(g)/\mathcal{I}(g)$ is always less than unity [20]. In a similar spirit, we can compare the ratio of the quantum Fisher information in the presence of thermal resources $\mathcal{I}_{\rm TH}(g)$ to the ideal postselected $\mathcal{I}_{\rm PS}(g)$.

The quantum Fisher information is evaluated from the Bures distance between ρ_g and ρ_{g+dg} [17], defined as $D_B^2(\rho_g, \rho_{g+dg}) = 2[1 - \sqrt{F(\rho_g, \rho_{g+dg})}]$, where ρ_g is the state containing the information about parameter g and $F(\rho_g, \rho_{g+dg})$ is the fidelity, defined as $F(\rho_1, \rho_2) = [\mathrm{tr}(\sqrt{\sqrt{\rho_1}\rho_2\sqrt{\rho_1}})]^2$. The quantum Fisher information as a measure of sensitivity is related to the curvature of the Bures distance at the parametric value g by the formula $\mathcal{I}(g) = -\partial_g^2 D_B^2(\rho_g, \rho_{g+dg})$. For the ideal WVA process, we assume $\langle B\rangle = 0$, and $\mathcal{I}_{\rm PS}(g)$ [27] is given by

$$\mathcal{I}_{\rm PS}(g) = 4P_s|\mathcal{A}_{\rm w}|^2[1 - |g\mathcal{A}_{\rm w}|^2\mathrm{Var}(B)], \tag{10}$$

where $\mathrm{Var}(B)$ is with respect to the initial meter state. The postselected Fisher information $\mathcal{I}_{\rm PS}(g)$ is always less than unity due to the rarity of the desired measurements. Now for nonideal measurements, $\mathcal{I}_{\rm TH}(g)$ is calculated as (see Appendix B)

$$\mathcal{I}_{\rm TH}(g) \approx 4P_M|\mathcal{A}'_{\rm w}|^2[1 - |g\mathcal{A}'_{\rm w}|^2\mathrm{Var}(B)]. \tag{11}$$

Here $\mathcal{A}'_{\rm w}$ is true weak value amplification, defined as

$$\mathcal{A}'_{\rm w} = \frac{\mathcal{A}_{\rm w}}{1+\delta_M}, \tag{12}$$

$$\text{where } \delta_M = \begin{cases} \frac{\bar{q}\bar{P}_s}{qP_s} & \text{for unbiased measurements,} \\ \frac{\bar{p}qP_s + p\bar{P}_s\bar{q}}{pqP_s + \bar{p}\bar{q}P_s} & \text{for noninvasive measurements.} \end{cases} \tag{13}$$

As $\delta_M > 0$ at any nonzero temperature, the true amplification is always less than the ideal amplification. The postselection probabilities P_M also depend on the system and pointer as

$$P_M = \begin{cases} qP_s & \text{for unbiased measurements,} \\ pqP_s + \bar{p}\bar{q}P_s & \text{for noninvasive measurements.} \end{cases} \tag{14}$$

In summary, WVA is, in general, affected by the rare postselection given in Eq. (4). In addition, the initial mixed state and the choice of nonideal measurements performed at the postselection further decrease the amplification given in Eq. (12). From Eqs. (12) and (13), we observe that the amplification due to the UB measurement depends only on the system temperature, and for NI measurements it depends on both system and pointer temperatures. To compare these measurement schemes in a concrete setting, we consider the original thought experiment [28] by Aharonov *et al.* in which the result of a measurement of a component of a spin-1/2 particle was amplified by 100, now implemented with thermal resources. Furthermore, we situate this thought experiment in the IBM transmon qubit and investigate the amplification obtained for different nonideal postmeasurements.

We initialize the system in a thermal state and perform the nonideal measurement to estimate the steady-state temperature to which the IBM transmon qubit has to be cooled to get desired amplification. The IBM transmon qubit works at the characteristic frequency of around 5–5.4 GHz [29] and also consists of a dilution refrigerator that can cool the system down to 15 mK [30]. We note that while we are taking 15 mK as the lower limit for the current discussion, the real lower limit of the temperature to which a given system can be cooled depends on hardware constraints which should be appropriately considered while applying our analysis to experiments. The original thought experiment [28] discussed consists of a system prepared in a pure state $\rho_i = |\downarrow\rangle\langle\downarrow|$. The system is then evolved by the Hamiltonian $A = \sigma_x$ and finally postselected onto the state $|\psi_f\rangle = \cos(\theta)|\uparrow\rangle + \sin(\theta)|\downarrow\rangle$, giving the amplification $\mathcal{A}_{\rm w} = \cot(\theta)$. With $\theta = 0.01$, the parameter g is amplified $\mathcal{A}_{\rm w} \approx 100$ times. Performing this experiment demands stringent cooling requirements. To demonstrate this, we simulated the nonideal amplification obtained with the WVA scheme performed on the IBM transmon setup as a function of the temperatures of the system and pointer. Figure 2 shows the simulation for the NI measurement, and Fig. 3 shows the simulation for the UB measurement. The amplification obtained from the NI measurement is affected by both system and pointer temperatures, as shown in Eq. (13). The pointer states prepared above 30 mK prove to be detrimental for weak value amplification ($\mathcal{A}'_{\rm w} < 1$) even for a system state prepared at very low temperature. For the UB measurement, the initial system state prepared below 52 mK shows an amplification ($\mathcal{A}'_{\rm w} > 1$), and states prepared below 20 mK attain near-desired amplification. This amplification is irrespective of the temperature at which the pointer states are prepared, as shown in Eq. (13). As cooling costs energy [8,9,31], the resource cost for UB measurements is much more favorable than for NI measurements.

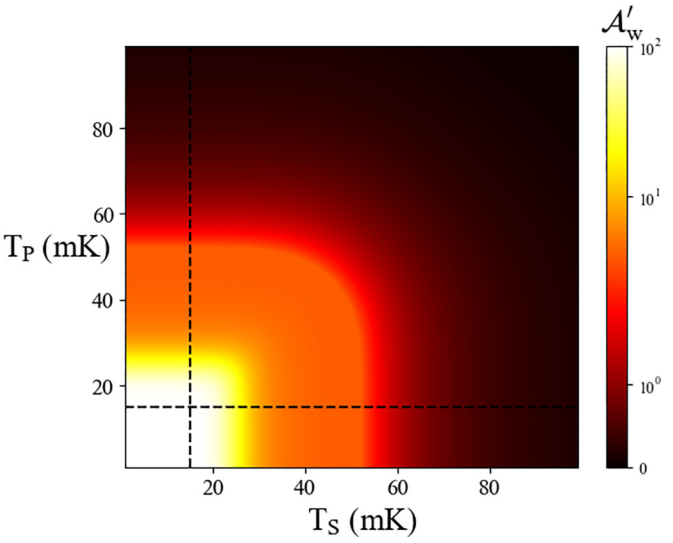

FIG. 2. Contour plot of true amplification for system and pointer qubits composed of transmons at $E_P = E_S = 5$ GHz for NI measurements. The amplification is denoted by the color bar and can be seen to depend on both the initial-state and pointer temperatures plotted along the two axes. The dotted line represents the lowest temperature achievable by the dilution refrigerator. The achievable amplification is hence the intersection of the region to the right of the vertical dashed line and above the horizontal dashed line.

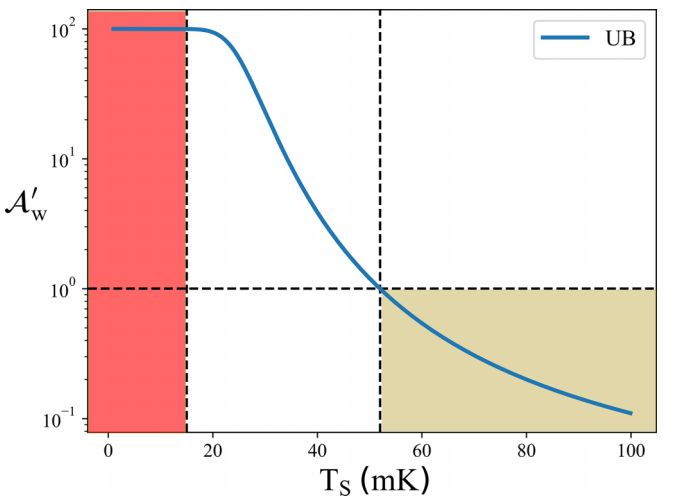

FIG. 3. True amplification plotted as a function of the system temperature for a UB measurement with $E_P = E_S = 5$ GHz. The amplification depends only on the initial-state temperature in the UB measurement as discussed in the text. The true amplification $\mathcal{A}'_{\rm w} < 1$ for $T_S > 52$ mK, which is shaded brown and denotes deamplification due to the effect of temperature. The red region shows the temperature range unattainable in the experiment considered in the text.

In summary, we can observe that UB measurements are favored over NI measurements, which can be concluded from the figure of merit given in Eq. (11). This observation is further supported by the resource requirements associated with cooling quantum systems. This is a consequence of properties of UB measurements, in which the pointer replicates the system statistics irrespective of its own temperature. From Eqs. (13) and (14) it can be observed that true amplification and postselection probability do not depend on pointer statistics, as also shown in Fig. 1. Hence, the UB measurements are preferred when getting the correct statistics of the system is more important according to the figure of merit. In contrast, there are metrology protocols which prioritize reduced states over measurement statistics. In the next section, we consider one such example and show how NI measurements have an operational advantage over UB measurements.

IV. SEQUENTIAL METROLOGY FAVORS NONINVASIVE MEASUREMENTS

While conveyer-belt models of metrology [32] imply that the initial state is an infinite free resource, sequential metrology schemes that prevent resetting account for the role played by the initial coherences of the state. The sequential metrology scheme without resetting involves initializing the probe state once, followed by cycles of evolution and measurement of the final state. This is different from repeated-interaction schemes in which an initial probe state interacts with the parameter repeatedly before being measured once [33]. Recently, a sequential metrological scheme without resetting was proposed to beat the shot-noise limit without exploiting entanglement resources in probe states [34]. A similar scheme was used in estimating the temperature of the thermal reservoir by sequentially measuring the probe states in contact with the reservoir without resetting [35]. In such settings, the statistics need to be preserved for the system and conveyed through a pointer before the next measurement. Simultaneously, the postmeasurement state of the system needs to be able to continue to acquire information about the unknown parameter, which is affected by the type of realistic measurement used. Hence, a natural question that arises is whether sequential metrology without resetting places a natural preference on statistics or reduced states. We now compare sequential metrology with different thermodynamically consistent measurements discussed before.

Once again, we consider the transmon qubit initially in the thermal state with a transition frequency of 5 GHz at temperature $\mathrm{T_S} = 100$ mK. The system is evolved according to the Hamiltonian $H = \theta\sigma_x$, acquiring an unknown phase θ whose inference proceeds through a measurement by correlating it with a pointer. As outlined above, the sequential nature of this metrology scheme is the repeated interaction and measurement. We start with a system initialized in state $\rho_{S,0}$ which will be evolved and measured repeatedly with measurement operators $M_{1,2} = [|\downarrow\rangle\langle\downarrow|, |\uparrow\rangle\langle\uparrow|]$ acting on the pointer state. Each sequence consists of a pair of unitary evolutions which gains phase, followed by a measurement event. There are N_s sequential measurements performed on each initialized system, and this whole sequence of measurements is repeated ν times for statistical inference. For instance, $\rho_{S,i}$ represents

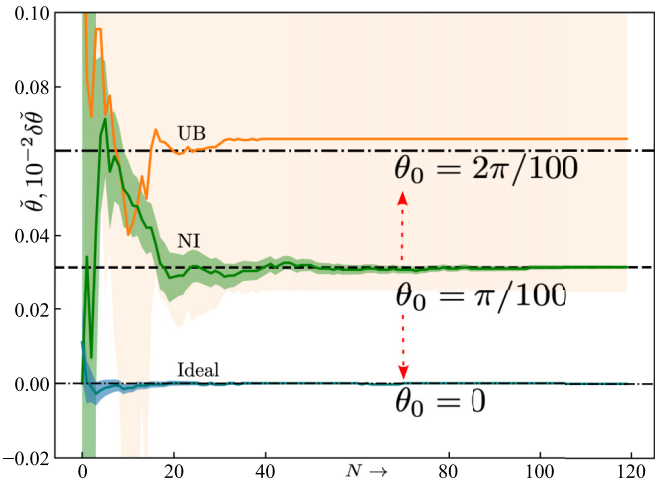

FIG. 4. Maximum-likelihood-estimation (MLE) average and standard deviation for a number of measurements for the case of sequential metrology without resetting. Here the system and pointer states taken to be at 5 GHz are prepared in the initial thermal state corresponding to $T_S = 100$ mK. The state of the system is evolved by the Hamiltonian $H = \theta\sigma_x$, where $\theta = \pi/100$ and is measured along the z direction. MLEs corresponding to the UB measurement (orange), NI measurement (green), and ideal measurement (teal) are presented alongside a dashed line that represents the true value ($\pi/100$). Note that the trajectories corresponding to UB measurements are displaced by $+\pi/100$, and likewise, the trajectories of ideal measurement are displaced by $-\pi/100$, as indicated on the plot for clarity. Note that the UB estimate converges to the wrong value, and its standard deviation, given by the orange shaded region, is large. On the other hand, the ideal and NI measurements converge to the correct mean with low standard deviations, and the ideal outperforms the NI measurement.

the initial system state at the ith step of the sequence of evolution and measurements. The total number of measurements performed $N_s\nu$ results in N sequences $\gamma^{(i)} = \{\nu_\uparrow^{(i)}/\nu, \nu_\downarrow^{(i)}/\nu\}$, which represent experimental frequencies. In the case of ideal measurements, since the system state and the pointer statistics are both unchanged at the end of the measurement, N_s copies of the ideal measurement statistics $\gamma_{\mathrm{id}}^{(i)}$ are received at the detectors. In contrast, the situation is different for nonideal measurements. In the case of NI measurements, while the reduced system state remains the same at the end of each measurement, the pointer statistics $\gamma_{NI}^{(i)}$ are slightly different owing to the finite temperature discussed to this point. This case is exactly reversed for UB measurements, where the reduced state of the system is modified at the end of each measurement, whereas the pointer statistics $\gamma_{UB}^{(i)}$ remains unaltered. Hence, each measurement considered above might acquire information about the unknown phase at a different rate. To study all three schemes fairly using the same analytical technique, we estimate the unknown phase by employing a maximum-likelihood estimator (MLE) [36] which considers all collected measurement statistics to infer the unknown parameter.

In Fig. 4 we present the MLE estimate of parameter $\check{\theta}$ as a function of the number of measurements N. The log-likelihood function $l(\theta) := \sum_\alpha \gamma_\alpha \log_e[p_\alpha(\theta)]$ is defined in

terms of the observed statistics γ and the parametrized probability distribution $p(\theta)$ corresponding to the outcome index by α. This likelihood function can also be seen as the second term in a Kullback-Liebler divergence $D[\gamma \| p(\theta)]$ and hence derives meaning as the minimization of a divergence between probability distributions. We note that for multiple measurements $\gamma^{(i)}$ resulting from potentially different parametrized probability distributions $p^{(i)}(\theta)$ defined as a function of the same unknown parameter θ, the divergence compares the product distributions of the statistics and the parametrized distributions, leading to a log-likelihood function $l(\theta) := \sum_i \sum_\alpha \gamma_\alpha^{(i)} \log_e[p_\alpha^{(i)}(\theta)]$. The estimate $\check{\theta}$ maximizes $l(\theta)$, and the standard deviation is computed via the curvature of the log-likelihood function as $\{-\mathbb{E}[\nabla^2 l(\check{\theta})]\}^{-\frac{1}{2}}$.

In Fig. 4, we estimate the parameter whose true value is $\theta = \pi/100$ using the MLE method for the sequential metrological scheme discussed above for ideal, NI, and UB measurements. In the case of ideal measurements, we observe that $\check{\theta}$ saturates to θ_{true} after a few measurements. Furthermore, the standard deviation in the estimate also converges to attainable sensitivity after a few iterations. This serves as a benchmark for the performance of the other two nonideal measurement schemes. On the other hand, the estimated value from the UB measurement saturates to an incorrect value. We understand this as a result of the reduced system state approaching the maximally mixed state after repeated measurements. For instance, the purity of the postmeasurement states after $N_s = 120$ measurements is ≈ 0.8 for the NI measurement, whereas it is ≈ 0.5 for the UB measurement up to numerical accuracy. Hence, its ability to acquire the correct information about the parameter deteriorates after each measurement. The standard deviation of the estimator is also very large for the same reason. Finally, for the NI measurement, the system state is unchanged after each measurement, so the estimated value converges to θ_{true}. The standard deviation of the estimator also approaches better sensitivity after a few measurements, but less than the ideal measurement case. In summary, NI measurements favor schemes such as repeated metrology without resetting. This is because preserving the statistics of the states after each measurement is more important for such schemes as it maximizes the figure of merit.

V. DISCUSSION AND CONCLUSION

An ideal measurement is thermodynamically inconsistent because it requires infinite resources. The inclusion of thermodynamics gives rise to two different realistic measurements, namely, UB and NI measurements. We showed that for the UB measurement, WVA shows better amplification by consuming fewer resources, which is the result of the pointer replicating system statistics. Due to this fact, the amplification depends only on the system temperature for the UB measurement and depends on both system and pointer temperatures for the NI measurement. We also considered a single-shot sequential metrological scheme in which the NI measurement shows an advantage over the UB measurement. This is because we considered a scheme without resetting the probe state, and we saw that preserving the purity of the reduced state of the system is important to the task of acquiring information about the phase over successive runs.

We discussed the strict constraints that thermodynamically consistent measurements place on quantum experiments, even though such experiments were performed before [25,37,38] and require some discussion. It should be noted that the imperfect correlation between the system and the pointer is a consequence of a full-rank finite-dimensional pointer at nonzero temperature. This analysis can hence be circumvented by the use of an infinite-dimension pointer [11] such as a harmonic oscillator or by cooling to a low enough temperature, as noted in Fig. 2. In reality, using infinite-dimensional pointers such as mechanical or light modes is not guaranteed, and further care has to be taken.

Hence, our analysis suggests that realistic metrological tasks with thermodynamically consistent measurements can be classified into two categories based on whether the pointer statistics or the reduced states of the system are important. Finally, we note that optimizing over other figures of merits might posit schemes which use UB and NI measurements together to achieve optimal performance. Our results hence contribute to the general task of designing realistic quantum metrology tasks with thermodynamically consistent resources and could guide such experimental design in the future.

ACKNOWLEDGMENTS

S.V. acknowledges support from the government of India DST-QUEST Grant No. DST/ICPS/QuST/Theme-4/2019 and discussions with R. Vijay and F. Binder.

APPENDIX A: QUANTUM FISHER INFORMATION DEPENDENCE ON PURITY

In this Appendix we briefly derive the form of the quantum Fisher information (QFI) as described in [39] and prove that for unitary parametrization, if the direction of the Bloch vector is kept the same, then the QFI increases with the increase in the purity of the state.

Consider the Bloch representation of a general **d**-level quantum system (qudit) as follows [39]:

$$\rho = \frac{1}{d}\mathbb{I}_d + \frac{1}{2}\sum_{i=1}^{d^2-1} \omega_i \hat{\eta}_i. \tag{A1}$$

Here $\mathbb{I}_d$ is a $d \times d$ identity operator, $\hat{\boldsymbol{\eta}} = \{\hat{\eta}_1, \hat{\eta}_2, \ldots, \hat{\eta}_{d^2-1}\}$ are the generators of the Lie algebra **su(d)**, and ω_i are the components of the Bloch vector $\boldsymbol{\omega} = (\omega_1, \omega_2, \ldots, \omega_{d^2-1})^T$.

Now if the system is evolved with a parameter-dependent unitary $U_\lambda = e^{-i(\boldsymbol{r}\cdot\hat{\boldsymbol{\eta}})\lambda}$, where $\boldsymbol{r}$ is a constant Bloch vector, we will get

$$\rho_\lambda = U_\lambda \rho U_\lambda^\dagger = \frac{1}{d}\mathbb{I}_d + \frac{1}{2}\sum_{i=1}^{d^2-1} \omega_i(\lambda)\hat{\eta}_i$$

$$\Rightarrow \rho_\lambda = \frac{1}{d}\mathbb{I}_d + \frac{1}{2}\boldsymbol{\omega}(\lambda)\cdot\hat{\boldsymbol{\eta}}. \tag{A2}$$

The purity of the state ρ_λ is given by $\mathrm{Tr}(\rho_\lambda^2) = \mathrm{Tr}(\rho^2) = (1/d + |\boldsymbol{\omega}|^2/2)$. The QFI for the state ρ_λ is defined as

$$\mathcal{I}_\lambda = \mathrm{Tr}\left(\rho_\lambda L_\lambda^2\right) = \mathrm{Tr}\left[(\partial_\lambda \rho_\lambda) L_\lambda\right]. \tag{A3}$$

Here L_λ is the symmetric logarithmic derivative (SLD) operator and is determined by

$$\partial_\lambda \rho_\lambda = \tfrac{1}{2}\{\rho_\lambda, L_\lambda\}, \tag{A4}$$

where $\{\cdot,\cdot\}$ is the anticommutator. To find L_λ we expand it in terms of $\mathfrak{su}(d)$ generators as follows:

$$L_\lambda = a\mathbb{I}_d + \boldsymbol{b}\cdot\hat{\boldsymbol{\eta}}. \tag{A5}$$

To determine a and vector $\boldsymbol{b} = \{b_i\}$ we use Eqs. (A2) and (A5) in Eq. (A4) to get

$$\begin{aligned}
&\frac{1}{2}[\partial_\lambda \boldsymbol{\omega}(\lambda)]\cdot\hat{\boldsymbol{\eta}} = \frac{1}{2}\{\rho, L\} = \frac{1}{2}\left(\left\{\frac{\mathbb{I}}{d}, a\mathbb{I} + \boldsymbol{b}\cdot\hat{\boldsymbol{\eta}}\right\}\left\{\frac{1}{2}\boldsymbol{\omega}(\lambda)\cdot\hat{\boldsymbol{\eta}}, a\mathbb{I}\right\} + \left\{\frac{1}{2}\boldsymbol{\omega}(\lambda)\cdot\hat{\boldsymbol{\eta}}, \boldsymbol{b}\cdot\hat{\boldsymbol{\eta}}\right\}\right)\\
&\Rightarrow \frac{1}{2}[\partial_\lambda \boldsymbol{\omega}(\lambda)]\cdot\hat{\boldsymbol{\eta}} = \frac{1}{d}[a + \boldsymbol{\omega}(\lambda)^{\mathrm{T}}\boldsymbol{b}]\mathbb{I} + \sum_{k=1}^{d^2-1}\left(\frac{1}{d}b_k + \frac{1}{2}a\omega_k(\lambda) + \frac{1}{2}\sum_{i,j=1}^{d^2-1} g_{ijk}\omega_i(\lambda)b_j\right)\hat{\eta}_k.
\end{aligned} \tag{A6}$$

Here g_{ijk} are the completely symmetric structure constants of the **su(d)** algebra, defined as

$$g_{ijk} = \tfrac{1}{4}\,\mathrm{Tr}(\{\hat{\eta}_i, \hat{\eta}_j\}\hat{\eta}_k). \tag{A7}$$

Now by comparing both sides of Eq. (A6) we get

$$\begin{aligned}
&a + \boldsymbol{\omega}(\lambda)^{\mathrm{T}}\boldsymbol{b} = 0,\\
&[\partial_\lambda \boldsymbol{\omega}(\lambda)]\cdot\hat{\boldsymbol{\eta}} = \frac{2}{d}\boldsymbol{b}\cdot\hat{\boldsymbol{\eta}} + (a\boldsymbol{\omega})\cdot\hat{\boldsymbol{\eta}} + (G\boldsymbol{b})\cdot\hat{\boldsymbol{\eta}},
\end{aligned} \tag{A8}$$

where G is a $d\times d$ matrix with elements defined as $G_{ij} = \sum_{k=1}^{d^2-1} g_{ijk}\omega_k(\lambda)$. To simplify Eq. (A8), we can find the value of a by writing L_λ in terms of eigenvalues and eigenvectors of ρ_λ [40,41] and comparing it to Eq. (A5). The parameterized state ρ_λ can be written in its eigenbasis, i.e., $\rho_\lambda = \sum_i C_i|\psi_i\rangle\langle\psi_i|$. Using this form of ρ_λ, the SLD operator L_λ can be written as

$$L_\lambda = 2\sum_{i,j}\frac{\langle\psi_i|\partial_\lambda\rho_\lambda|\psi_j\rangle}{C_i + C_j}|\psi_i\rangle\langle\psi_j|, \tag{A9}$$

and the summation goes over all i, j such that $C_i + C_j \neq 0$. For unitary evolution, we have $\partial_\lambda\rho_\lambda = -i[\boldsymbol{r}\cdot\hat{\boldsymbol{\eta}}, \rho_\lambda]$; using it in Eq. (A9) will give

$$L_\lambda = -2i\sum_{i,j}\frac{\langle\psi_i|[\boldsymbol{r}\cdot\hat{\boldsymbol{\eta}}, \rho_\lambda]|\psi_j\rangle}{C_i + C_j}|\psi_i\rangle\langle\psi_j|$$

or

$$L_\lambda = 2i\sum_{i,j}\frac{\langle\psi_i|\boldsymbol{r}\cdot\hat{\boldsymbol{\eta}}|\psi_j\rangle(C_i - C_j)}{C_i + C_j}|\psi_i\rangle\langle\psi_j|. \tag{A10}$$

Comparing Eq. (A10) with Eq. (A5), we get

$$a\mathbb{I}_d + \boldsymbol{b}\cdot\hat{\boldsymbol{\eta}} = 2i\sum_{i,j}\frac{\langle\psi_i|\boldsymbol{r}\cdot\hat{\boldsymbol{\eta}}|\psi_j\rangle(C_i - C_j)}{C_i + C_j}|\psi_i\rangle\langle\psi_j|. \tag{A11}$$

Taking the trace on both sides in Eq. (A11) gives

$$\begin{aligned}
&\mathrm{Tr}(a\mathbb{I}_d + \boldsymbol{b}\cdot\hat{\boldsymbol{\eta}})\\
&= \mathrm{Tr}\left(2i\sum_{i,j}\frac{\langle\psi_i|\boldsymbol{r}\cdot\hat{\boldsymbol{\eta}}|\psi_j\rangle(C_i - C_j)}{C_i + C_j}|\psi_i\rangle\langle\psi_j|\right)\\
&\Rightarrow ad = 2i\sum_{i,j}\frac{\langle\psi_i|\boldsymbol{r}\cdot\hat{\boldsymbol{\eta}}|\psi_j\rangle(C_i - C_j)}{C_i + C_j}\delta_{ij}\\
&\Rightarrow ad = 0 \text{ or } a = 0.
\end{aligned} \tag{A12}$$

Using this, we can simplify Eq. (A8) as

$$\begin{aligned}
a &= \boldsymbol{\omega}(\lambda)^{\mathrm{T}}\boldsymbol{b} = 0,\\
\partial_\lambda\boldsymbol{\omega}(\lambda) &= \left(\frac{2}{d}\mathbb{I} + G\right)\boldsymbol{b}\\
\Rightarrow \boldsymbol{b} &= \left(\frac{2}{d}\mathbb{I} + G\right)^{-1}[\partial_\lambda\boldsymbol{\omega}(\lambda)].
\end{aligned} \tag{A13}$$

Now from Eqs. (A5) and (A3) we can determine the Fisher information to be $\mathcal{I}_\lambda = [\partial_\lambda\boldsymbol{\omega}(\lambda)]^{\mathrm{T}}\boldsymbol{b}$. Using the value of $\boldsymbol{b}$ from Eq. (A13), we get

$$\mathcal{I}_\lambda = [\partial_\lambda\boldsymbol{\omega}(\lambda)]^{\mathrm{T}}\left(\frac{2}{d}\mathbb{I} + G\right)^{-1}[\partial_\lambda\boldsymbol{\omega}(\lambda)]. \tag{A14}$$

The inverse of the matrix may not exist in Eq. (A14); hence, we define the inverse only in support of the matrix. Now we can take $\boldsymbol{\omega} = |\boldsymbol{\omega}|(\hat{\omega}_1, \hat{\omega}_2, \ldots, \hat{\omega}_{d^2-1})^T = |\boldsymbol{\omega}|\hat{\boldsymbol{\omega}}$, where $|\boldsymbol{\omega}|$ is the length of the Bloch vector and $\{\hat{\omega}_i\}$ are the components of the unit vector. The matrix G can then be written as $G = |\boldsymbol{\omega}|\tilde{G}$, and elements of $\tilde{G}$ will be given as $\tilde{G}_{ij} = \sum_{k=1}^{d^2-1} g_{ijk}\hat{\omega}_k(\lambda)$. We note that the matrix $\tilde{G}$ is the same for any two Bloch vectors with same-direction cosines. Let the spectral decomposition of $\tilde{G}$ be $\tilde{G} = \sum_i \tilde{g}_i\boldsymbol{v}_i\boldsymbol{v}_i^{\mathrm{T}}$, where $\{\tilde{g}_i\}$ and $\{\boldsymbol{v}_i\}$ are eigenvalues and eigenvectors of $\tilde{G}$, respectively. The QFI can then be expressed as

$$\mathcal{I}_\lambda = [\partial_\lambda\boldsymbol{\omega}(\lambda)]^{\mathrm{T}}\sum_{i=1}^{d^2-1}\frac{\boldsymbol{v}_i\boldsymbol{v}_i^{\mathrm{T}}}{2/d + |\boldsymbol{\omega}|\tilde{g}_i}[\partial_\lambda\boldsymbol{\omega}(\lambda)]. \tag{A15}$$

Since we define the inverse only in support of the matrix, we sum over only the terms that are well defined in Eq. (A15), i.e., $2/d + |\boldsymbol{\omega}|\tilde{g}_i \neq 0$.

Now for unitary transformation U_λ, we have

$$\begin{aligned}\partial_\lambda \rho_\lambda &= -i[\boldsymbol{r}\cdot\hat{\boldsymbol{\eta}}, \rho_\lambda] \\ &= -i\left[\boldsymbol{r}\cdot\hat{\boldsymbol{\eta}}, \frac{1}{d}\mathbb{I}_d + \frac{1}{2}\boldsymbol{\omega}(\lambda)\cdot\hat{\boldsymbol{\eta}}\right] \\ \Rightarrow \partial_\lambda \boldsymbol{\omega}(\lambda)\cdot\hat{\boldsymbol{\eta}} &= \frac{1}{2}\sum_{i,j=1}^{d^2-1} r_i\omega_j(\lambda)[\hat{\eta}_i, \hat{\eta}_j] \\ \Rightarrow \sum_{k=1}^{d^2-1}\partial_\lambda\omega_k(\lambda)\hat{\eta}_k &= \sum_{k=1}^{d^2-1}\sum_{i,j=1}^{d^2-1} r_i\omega_j(\lambda)f_{ijk}\hat{\eta}_k \\ \Rightarrow \partial_\lambda\omega_k(\lambda) &= \sum_{i,j=1}^{d^2-1} r_i\omega_j(\lambda)f_{ijk} = |\boldsymbol{\omega}|\sum_{i,j=1}^{d^2-1} r_i\hat{\omega}_j(\lambda)f_{ijk} \\ \Rightarrow \partial_\lambda\omega_k(\lambda) &= |\boldsymbol{\omega}|\partial_\lambda\hat{\omega}_k(\lambda) \\ &\text{or} \\ \Rightarrow \partial_\lambda\boldsymbol{\omega}(\lambda) &= |\boldsymbol{\omega}|\partial_\lambda\hat{\boldsymbol{\omega}}(\lambda). \end{aligned} \tag{A16}$$

Here the term f_{ijk} denotes completely antisymmetric structure constants of the **su(d)** algebra, defined as

$$f_{ijk} = \tfrac{1}{4}\,\mathrm{Tr}([\hat{\eta}_i, \hat{\eta}_j]\hat{\eta}_k). \tag{A17}$$

Using Eq. (A16) in Eq. (A15), we get

$$\mathcal{I}_\lambda = \sum_{i=1}^{d^2-1}\frac{\left|\boldsymbol{v}_i^{\mathrm{T}}[\partial_\lambda\hat{\boldsymbol{\omega}}(\lambda)]\right|^2|\boldsymbol{\omega}|^2}{2/d + |\boldsymbol{\omega}|\tilde{g}_i}. \tag{A18}$$

Hence, from Eq. (A18) we can say that if the unknown parameter (λ) is acquired from unitary evolution, then the QFI of this process depends on the length of the Bloch vector, which depends on the purity of the state. To see how the QFI changes with purity, we evaluate the first derivative of QFI with respect to $|\boldsymbol{\omega}|$ as follows:

$$\begin{aligned}\frac{d\mathcal{I}_\lambda}{d(|\boldsymbol{\omega}|)} &= \sum_{i=1}^{d^2-1}\left|\boldsymbol{v}_i^{\mathrm{T}}[\partial_\lambda\hat{\boldsymbol{\omega}}(\lambda)]\right|^2\frac{4|\boldsymbol{\omega}|/d + \tilde{g}_i|\boldsymbol{\omega}|^2}{(2/d + |\boldsymbol{\omega}|\tilde{g}_i)^2} \\ &= \frac{\mathcal{I}_\lambda}{|\boldsymbol{\omega}|} + \sum_{i=1}^{d^2-1}\frac{2d\left|\boldsymbol{v}_i^{\mathrm{T}}[\partial_\lambda\hat{\boldsymbol{\omega}}(\lambda)]\right|^2|\boldsymbol{\omega}|}{(2 + d|\boldsymbol{\omega}|\tilde{g}_i)^2}. \end{aligned} \tag{A19}$$

Since QFI is always positive, from Eq. (A19) we can say that $\frac{d\mathcal{I}_\lambda}{d(|\boldsymbol{\omega}|)} \geqslant 0\ \forall|\boldsymbol{\omega}| > 0$. Therefore, if the state ρ acquires the phase related to the unknown parameter λ via unitary transformation, from Eqs. (A18) and (A19) we can conclude that the QFI increases with an increase in the purity of the state provided the direction cosines of the parameter-independent Bloch vector of the initial state are kept constant.

APPENDIX B: PROOF OF NONIDEAL WEAK VALUE

In this Appendix, we evaluate the kicked state for nonideal measurements. Consider the initial state of the system prepared in the thermal state,

$$\rho_s = q|\psi_i\rangle\langle\psi_i| + \bar{q}|\psi_i^\perp\rangle\langle\psi_i^\perp|, \tag{B1}$$

where $\tilde{q}/(1-\tilde{q}) = \exp(-\beta E_s)$. The combination of the system and meter state is

$$\begin{aligned}\rho_{sm} = {}& \bar{q}e^{-igA\otimes B}(|\psi_i\rangle\langle\psi_i|\otimes\rho_m)e^{igA\otimes B} \\ &+ \bar{q}e^{-igA\otimes B}(|\psi_i^\perp\rangle\langle\psi_i^\perp|\otimes\rho_m)e^{igA\otimes B}. \end{aligned} \tag{B2}$$

Using the Gram-Schmidt orthogonalization procedure and writing the initial state in terms of final states, we get

$$\begin{aligned}|\psi_i\rangle &= a|\psi_f\rangle + b|\psi_f^\perp\rangle, \\ |\psi_i^\perp\rangle &= b^*|\psi_f\rangle - a^*|\psi_f^\perp\rangle, \end{aligned} \tag{B3}$$

where $a = \langle\psi_f|\psi_i\rangle$. Finally,

$$\begin{aligned}|\psi_i\rangle\langle\psi_i| = {}& |a|^2|\psi_f\rangle\langle\psi_f| + ab^*|\psi_f\rangle\langle\psi_f^\perp| \\ &+ a^*b|\psi_f^\perp\rangle\langle\psi_f| + |b|^2|\psi_f^\perp\rangle\langle\psi_f^\perp| \end{aligned} \tag{B4}$$

and

$$\begin{aligned}|\psi_i^\perp\rangle\langle\psi_i^\perp| = {}& |b|^2|\psi_f\rangle\langle\psi_f| - ab^*|\psi_f\rangle\langle\psi_f^\perp| \\ &- a^*b|\psi_f^\perp\rangle\langle\psi_f| + |a|^2|\psi_f^\perp\rangle\langle\psi_f^\perp|. \end{aligned} \tag{B5}$$

The total system-meter state can be rewritten in terms of the final state and the state orthogonal to the final state,

$$\begin{aligned}\rho_{sm} = {}& q[(|a|^2|\psi_f\rangle\langle\psi_f| + |b|^2|\psi_f^\perp\rangle\langle\psi_f^\perp|)\otimes\rho_m - ig(ba^*|\psi_f\rangle\langle\psi_f| - ab^*|\psi_f^\perp\rangle\langle\psi_f^\perp|)\otimes B\rho_m + ig(a^*b|\psi_f^\perp\rangle\langle\psi_f^\perp| \\ &- ab^*|\psi_f\rangle\langle\psi_f|)\otimes\rho_m B] + \bar{q}[(|b|^2|\psi_f\rangle\langle\psi_f| + |a|^2|\psi_f^\perp\rangle\langle\psi_f^\perp|)\otimes\rho_m + ig(ba^*|\psi_f\rangle\langle\psi_f| - ab^*|\psi_f^\perp\rangle\langle\psi_f^\perp|)\otimes B\rho_m \\ &- ig(ab^*|\psi_f^\perp\rangle\langle\psi_f^\perp| - a^*b|\psi_f\rangle\langle\psi_f|)\otimes\rho_m B] + \text{ off-diagonal terms}. \end{aligned} \tag{B6}$$

Here and below off-diagonal terms do not appear in the calculations because they are eliminated after measurement. Now we take a thermal pointer state and correlate it with the system only in a system-meter state by using either the unbiased method or noninvasive method. The correlation matrix for the unbiased method is

$$U_{\mathrm{UB}} = \begin{bmatrix}1&0&0&0\\0&0&1&0\\0&0&0&1\\0&1&0&0\end{bmatrix}, \tag{B7}$$

and the correlation matrix for the noninvasive method is

$$U_{\mathrm{NI}} = \begin{bmatrix}1&0&0&0\\0&0&0&1\\0&0&1&0\\0&1&0&0\end{bmatrix}. \tag{B8}$$

Then correlating the joint system and meter with the evolution gives

$$\rho_{psm} = U_{\mathrm{UB/NI}}(\rho_p\otimes\rho_{sm})U_{\mathrm{UB/NI}}^\dagger. \tag{B9}$$

For the unbiased method, the correlated state is

$$\Psi^{ps}(\rho_{psm}) = pP_s\bar{q}|\psi_f\rangle\langle\psi_f| \otimes |\psi_f\rangle\langle\psi_f| \otimes \eta_1 + p\bar{P}_s\bar{q}|\psi_f\rangle\langle\psi_f| \otimes |\psi_f\rangle\langle\psi_f| \otimes \eta_2 + \bar{p}P_s\bar{q}|\psi_f\rangle\langle\psi_f| \otimes |\psi_f^{\perp}\rangle\langle\psi_f^{\perp}| \otimes \eta_1 + \bar{p}\bar{P}_s\bar{q}|\psi_f\rangle\langle\psi_f| \otimes |\psi_f^{\perp}\rangle\langle\psi_f^{\perp}| \otimes \eta_2 + \text{ off-diagonal terms.} \tag{B10}$$

For the NI measurement, the correlated state is

$$\Psi^{ps}(\rho_{psm}) = pP_s\bar{q}|\psi_f\rangle\langle\psi_f| \otimes |\psi_f\rangle\langle\psi_f| \otimes \eta_1 + p\bar{P}_s\bar{q}|\psi_f\rangle\langle\psi_f| \otimes |\psi_f\rangle\langle\psi_f| \otimes \eta_2 + \bar{p}\bar{P}_s\bar{q}|\psi_f\rangle\langle\psi_f| \otimes |\psi_f^{\perp}\rangle\langle\psi_f^{\perp}| \otimes \eta_1 + \bar{p}P_s\bar{q}|\psi_f\rangle\langle\psi_f| \otimes |\psi_f^{\perp}\rangle\langle\psi_f^{\perp}| \otimes \eta_2 + \text{ off-diagonal terms,} \tag{B11}$$

where $\eta_1 = \exp(-ig\mathcal{A}_w B)\rho_m \exp(ig\mathcal{A}_w B)$ and $\eta_2 = \exp[-i(g/\mathcal{A}_w)B]\rho_m \exp[+i(g/\mathcal{A}_w)B]$, such that $(g/\mathcal{A}_w) \ll g\mathcal{A}_w \ll 1$.

Finally, measurement in pointer onto $|\psi_f\rangle$ state, the post-measurement meter state for the UB measurement is

$$\rho_m^{\mathrm{PS(UB)}} = \mathrm{Tr}_p\left(\Psi_{\mathrm{pm}}^{\mathrm{unb}}\right) = (qP_s)\eta_1 + (\bar{P}_s\bar{q})\eta_2, \tag{B12}$$

and that for the NI measurement is

$$\rho_m^{\mathrm{PS(NI)}} = \mathrm{Tr}_p\left(\Psi_{\mathrm{pm}}^{\mathrm{ni}}\right) = (pqP_s\eta_1 + \bar{p}\bar{q}P_s\tilde{\eta}_1) + (p\bar{P}_s\bar{q} + \bar{p}q\bar{P}_s)\eta_2, \tag{B13}$$

where $\tilde{\eta}_1 = \exp(ig\mathcal{A}_w B)\rho_m \exp(-ig\mathcal{A}_w B)$, which is a Gaussian centered at $x = -g\mathcal{A}_w$.

We see that the amplification will be better for the UB measurement compared to the NI measurement because the accurate amplification will be a weighted average of the spread in the meter space. For the UB measurement, the weighted average lies between $x = 0$ and $x = g\mathcal{A}_w$. For the NI measurement, the weighted average is close to $x = 0$. If we imagine the meter state is a Gaussian function in the position basis, we see two Gaussians, one centered at $x = 0$ due to η_2 and another Gaussian centered at $x = g\mathcal{A}_w$ due to η_1.

Now we calculate the Fisher information for a nonideal measurement and compare it to Fisher information obtained from an ideal measurement. The postselected state for a nonideal measurement state can be rewritten as

$$\rho(g) = P_M(e^{-ig\mathcal{A}_w B}\rho_m e^{ig\mathcal{A}_w B}) + P_M\delta_M\rho_m. \tag{B14}$$

Now diagonalizing Eq. (B14) so that we can calculate the Bures distance easily,

$$\rho(g) = \frac{P_M}{2}[|g\mathcal{A}_w|^2\frac{2\delta_M}{\delta_M+1}|\psi_1\rangle\langle\psi_1| + (\delta_M+1)\frac{|g\mathcal{A}_w|^2}{\delta_M+1}|\psi_2\rangle\langle\psi_2|]. \tag{B15}$$

Now the Bures distance can be calculated from the fidelity between ρ_g and ρ_{g+dg},

$$F(\rho_g, \rho_{g+dg}) = |g\mathcal{A}_w||(g+dg)\mathcal{A}_w|\frac{\delta_M}{\delta_M+1} + (\delta_M+1)\sqrt{[1+|g\mathcal{A}_w/(\delta_M+1)|^2]} \times \sqrt{[1+|(g+dg)\mathcal{A}_w/\delta_M+1|^2]}. \tag{B16}$$

Computing the negative second derivative of g of the Bures distance gives us the Fisher information:

$$\mathcal{I}(g) = -\partial_g^2\{2[1-F(\rho_g, \rho_{g+dg})]\}, \tag{B17}$$

$$\mathcal{I}_{\mathrm{TH}}(g) = 4P_M|\mathcal{A}_w'|^2(1-|g\mathcal{A}_w'|^2), \tag{B18}$$

where the weak value is

$$\mathcal{A}_w' = \frac{\mathcal{A}_w}{1+\delta_M} \tag{B19}$$

and δ_M is

$$\delta_M = \begin{cases} \frac{\bar{q}\bar{P}_s}{qP_s} & \text{for the unbiased measurement,} \\ \frac{p\bar{P}_s\bar{q}+\bar{p}q\bar{P}_s}{pqP_s+\bar{p}\bar{q}P_s} & \text{for the noninvasive measurement} \end{cases} \tag{B20}$$

and P_M is

$$P_M = \begin{cases} qP_s & \text{for the unbiased measurement,} \\ pqP_s + \bar{p}\bar{q}P_s & \text{for the noninvasive measurement.} \end{cases} \tag{B21}$$

These are Eqs. (10)–(14) in the main text. The amplification is bad for both noninvasive and unbiased measurements compared to an ideal measurement. If we compare the NI method with the UB method, the Fisher information obtained from the UB measurement is better than that from the other method because the amplification depends only on the system purity, not on the pointer purity. In the UB measurement, the pointer replicates the system statistics, which is more important in a weak value amplification procedure. The NI procedure preserves only the states of the system, and the system statistics are changed; hence, we get better amplification through the UB measurement procedure compared to the NI measurement.

[1] V. Giovannetti, S. Lloyd, and L. Maccone, Nat. Photon. **5**, 222 (2011).

[2] J. A. H. Nielsen, J. S. Neergaard-Nielsen, T. Gehring, and U. L. Andersen, Phys. Rev. Lett. **130**, 123603 (2023).

[3] A. Luis, Phys. Rev. A **95**, 032113 (2017).
[4] S. Bandyopadhyay, S. Halder, and M. Nathanson, Phys. Rev. A **94**, 022311 (2016).
[5] K. M. R. Audenaert, J. Calsamiglia, R. Muñoz Tapia, E. Bagan, L. Masanes, A. Acin, and F. Verstraete, Phys. Rev. Lett. **98**, 160501 (2007).
[6] L. Masanes and J. Oppenheim, Nat. Commun. **8**, 14538 (2017).
[7] H. Wilming and R. Gallego, Phys. Rev. X **7**, 041033 (2017).
[8] F. Clivaz, R. Silva, G. Haack, J. B. Brask, N. Brunner, and M. Huber, Phys. Rev. Lett. **123**, 170605 (2019).
[9] A. E. Allahverdyan, K. V. Hovhannisyan, D. Janzing, and G. Mahler, Phys. Rev. E **84**, 041109 (2011).
[10] D. Reeb and M. M. Wolf, New J. Phys. **16**, 103011 (2014).
[11] Y. Guryanova, N. Friis, and M. Huber, Quantum **4**, 222 (2020).
[12] J. Von Neumann, *Mathematical Foundations of Quantum Mechanics*, Princeton Landmarks in Mathematics and Physics Vol. 53 (Princeton University Press, Princeton, NJ, 2018), pp. 283–288.
[13] G. Lüders, Ann. Phys. (Berlin, Ger.) **518**, 663 (2006).
[14] M. H. Mohammady and T. Miyadera, Phys. Rev. A **107**, 022406 (2023).
[15] P. Busch, P. J. Lahti, and P. Mittelstaedt, The quantum theory of measurement, in *The Quantum Theory of Measurement* (Springer, Berlin, 1996), pp. 25–90.
[16] T. Debarba, G. Manzano, Y. Guryanova, M. Huber, and N. Friis, New J. Phys. **21**, 113002 (2019).
[17] S. L. Braunstein and C. M. Caves, Phys. Rev. Lett. **72**, 3439 (1994).
[18] J. S. Sidhu and P. Kok, AVS Quantum Sci. **2**, 014701 (2020).
[19] L. Vaidman, Philos. Trans. R. Soc. A **375**, 20160395 (2017).
[20] S. Pang, J. Dressel, and T. A. Brun, Phys. Rev. Lett. **113**, 030401 (2014).
[21] G. C. Knee and E. M. Gauger, Phys. Rev. X **4**, 011032 (2014).
[22] A. N. Jordan, J. Martínez-Rincón, and J. C. Howell, Phys. Rev. X **4**, 011031 (2014).
[23] A. Feizpour, X. Xing, and A. M. Steinberg, Phys. Rev. Lett. **107**, 133603 (2011).
[24] G. Strübi and C. Bruder, Phys. Rev. Lett. **110**, 083605 (2013).
[25] D. J. Starling, P. B. Dixon, A. N. Jordan, and J. C. Howell, Phys. Rev. A **82**, 063822 (2010).
[26] S. Haroche, Rev. Mod. Phys. **85**, 1083 (2013).
[27] G. B. Alves, B. M. Escher, R. L. de Matos Filho, N. Zagury, and L. Davidovich, Phys. Rev. A **91**, 062107 (2015).
[28] Y. Aharonov, D. Z. Albert, and L. Vaidman, Phys. Rev. Lett. **60**, 1351 (1988).
[29] J. M. Chow, S. J. Srinivasan, E. Magesan, A. D. Córcoles, D. W. Abraham, J. M. Gambetta, and M. Steffen, Proc. SPIE **9500**, 95001G (2015).
[30] J. M. Hornibrook, J. I. Colless, I. D. Conway Lamb, S. J. Pauka, H. Lu, A. C. Gossard, J. D. Watson, G. C. Gardner, S. Fallahi, M. J. Manfra, and D. J. Reilly, Phys. Rev. Appl. **3**, 024010 (2015).
[31] S. Vinjanampathy and J. Anders, Contemp. Phys. **57**, 545 (2016).
[32] B. Peaudecerf, C. Sayrin, X. Zhou, T. Rybarczyk, S. Gleyzes, I. Dotsenko, J. M. Raimond, M. Brune, and S. Haroche, Phys. Rev. A **87**, 042320 (2013).
[33] B. L. Higgins, D. W. Berry, S. D. Bartlett, H. M. Wiseman, and G. J. Pryde, Nature (London) **450**, 393 (2007).
[34] V. Montenegro, G. S. Jones, S. Bose, and A. Bayat, Phys. Rev. Lett. **129**, 120503 (2022).
[35] D. Burgarth, V. Giovannetti, A. N. Kato, and K. Yuasa, New J. Phys. **17**, 113055 (2015).
[36] M. Hayashi, S. Vinjanampathy, and L. C. Kwek, J. Phys. B **52**, 015503 (2019).
[37] G. C. Knee, J. Combes, C. Ferrie, and E. M. Gauger, Quantum Meas. Quantum Metrol. **3**, 32 (2016).
[38] C. Krafczyk, A. N. Jordan, M. E. Goggin, and P. G. Kwiat, Phys. Rev. Lett. **126**, 220801 (2021).
[39] W. Zhong, Z. Sun, J. Ma, X. Wang, and F. Nori, Phys. Rev. A **87**, 022337 (2013).
[40] J. Liu, J. Chen, X.-X. Jing, and X. Wang, J. Phys. A **49**, 275302 (2016).
[41] M. G. Paris, Int. J. Quantum Inf. **07**, 125 (2009).